Supporting Information

The Relative Efficiencies of $CpM(CO)_nCH_3$ and $CpM(CO)_nPh$ Complexes in Photoinduced DNA Cleavage

Debra L. Mohler,* E. Keller Barnhardt, and Allison L. Hurley

Department of Chemistry, Emory University, 1515 Pierce Dr., Atlanta, Georgia 30322

Plasmid relaxation by $[CpW(CO)_3]_2$.

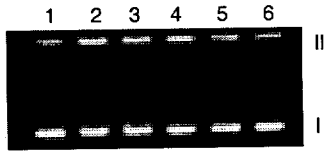

Figure S1. Relaxation of pBR322 DNA (30 μM/bp in 10% DMSO/20 mM Tris buffer, pH 8) by $[CpW(CO)_3]_2$. Lane 1, DNA alone; lanes 2—6, DNA + complex (3600, 1800, 900, 450, and 225 μM). Reactions in lane 2—6 were irradiated with Pyrex-filtered light from a 450 W medium pressure mercury arc lamp for 20 minutes.

Plasmid relaxation by $[CpFe(CO)_2]_2$.

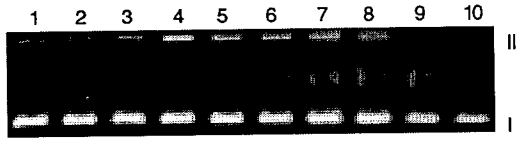

Figure S2. Relaxation of pBR322 DNA (30 μM/bp in 10% DMSO/20 mM Tris buffer, pH 8) by $[CpFe(CO)_2]_2$. Lanes 1 and 3, DNA alone; lanes 2 and 4—10, DNA + complex (90, 90, 45, 23, 11 ,5.6, 2.8, and 1.4 μM). Reactions in lanes 3—10 were irradiated with Pyrex-filtered light from a 450 W medium pressure mercury arc lamp for 20 minutes.

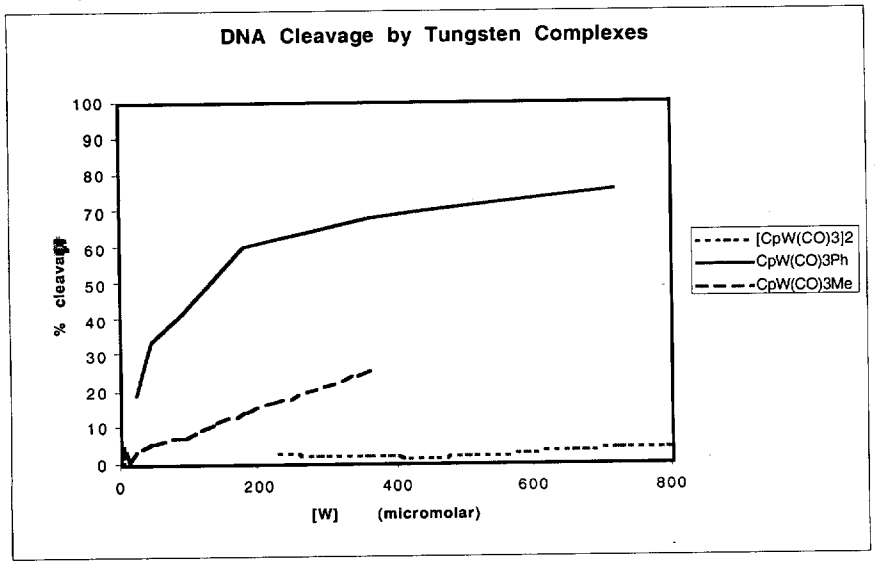

Figure S3. Plot of percent relaxation of pBR322 DNA (30 μM/bp in 10% DMSO/20 mM Tris buffer, pH 8) by $[CpW(CO)_3]_2$, $CpW(CO)_3Me$, and $CpW(CO)_3Ph$ *vs* concentration of tungsten species. To obtain value for % cleavage, the highest amount of form II observed in control lanes was subtracted from the sum of % form III and % form II for each concentration.

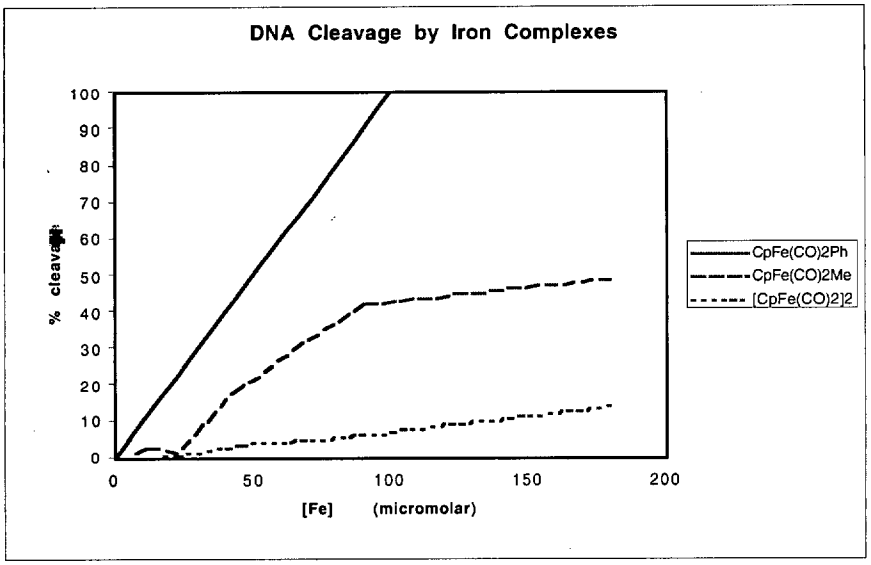

Figure S4. Plot of percent relaxation of pBR322 DNA (30 μM/bp in 10% DMSO/20 mM Tris buffer, pH 8) by $[CpFe(CO)_2]_2$, $CpFe(CO)_3Me$, and $CpFe(CO)_3Ph$ *vs* concentration of iron species. To obtain value for % cleavage, the highest amount of form II observed in control lanes was subtracted from the sum of % form III and % form II for each concentration. Graphs were prepared with Microsoft Excel.

Plasmid Assay Quantitation Data. The bands in the scanned gels were quantitated with the NIH ImageJ program to give the following data:

pBR322 cleavage by $CpW(CO)_3C_6H_5$ (Figure 1a):

Lane	$CpW(CO)_3C_6H_5$ (μM)	Form I (%)	Form II (%)	Form III (%)
1 (control)		93.5	6.5	0.0
2 (control)	360	82.1	17.9	0.0
3 (control)		84.7	15.3	0.0
4	360	56.7	63.3	0.0
5	180	67.9	32.1	0.0
6	90	75.0	25.0	0.0
7	45	76.5	23.5	0.0
8	22.5	78.7	21.3	0.0
9	11.3	81.8	18.2	0.0
10	5.6	77.1	22.9	0.0
11	2.8	81.7	18.3	0.0
12	1.4	82.0	18.0	0.0

pBR322 cleavage by $CpFe(CO)_2CH_3$ (Figure 1b):

Lane	$CpFe(CO)_2CH_3$ (μM)	Form I (%)	Form II (%)	Form III (%)
1 (control)		91.9	8.1	0.0
2 (control)	360	83.7	16.3	0.0
3 (control)		91.2	8.8	0.0
4	360	15.8	73.6	10.6
5	180	35.0	57.2	7.8
6	90	41.5	55.2	3.3
7	45	64.1	34.5	1.4
8	22.5	82.6	17.4	0.0
9	11.3	81.1	18.9	0.0
10	5.6	87.2	12.8	0.0
11	2.8	87.3	12.7	0.0
12	1.4	91.3	8.7	0.0

pBR322 cleavage by $CpFe(CO)_2C_6H_5$ (Figure 1c):

Lane	$CpFe(CO)_2C_6H_5$ (μM)	Form I (%)	Form II (%)	Form III (%)
1 (control)		73.2	26.8	0.0
2 (control)	360	71.3	28.7	0.0
3 (control)		71.4	28.6	0.0
4	360	0.0	0.0	0.0
5	180	0.0	0.0	0.0
6	90	0.0	0.0	0.0
7	45	0.0	0.0	0.0
8	22.5	0.0	60.4	39.6
9	11.3	8.9	80.5	10.6
10	5.6	66.3	33.7	0.0
11	2.8	65.9	34.1	0.0
12	1.4	79.8	20.2	0.0

pBR322 cleavage by $CpW(CO)_3CH_3$ (data from Figure 1 of reference #2):

Lane	$CpW(CO)_3CH_3$ (μM)	Form I (%)	Form II (%)	Form III (%)
1 (control)		99.1	0.9	0.0
2 (control)		96.3	3.7	0.0
3 (control)	720	96.0	4.0	0.0
4	720	20.6	79.4	0.0
5	360	28.5	71.5	0.0
6	180	36.6	63.4	0.0
7	90	55.0	45.0	0.0
8	45	62.4	37.6	0.0
9	22.5	77.5	22.5	0.0

pBR322 cleavage by $[CpW(CO)_3]_2$ (Figure S1):

Lane	$[CpW(CO)_3]_2$ (μM)	Form I (%)	Form II (%)	Form III (%)
1 (control)		83.5	16.5	0.0
2	3600	68.2	31.8	0.0
3	1800	71.2	28.8	0.0
4	900	77.9	22.1	0.0
5	450	82.2	17.8	0.0
6	225	80.6	19.4	0.0

pBR322 cleavage by $[CpFe(CO)_2]_2$ (Figure S2):

Lane	$[CpFe(CO)_2]_2$ (μM)	Form I (%)	Form II (%)	Form III (%)
1 (control)		88.2	11.8	0.0
2 (control)		94.3	5.7	0.0
3 (control)	90	90.2	9.8	0.0
4	90	74.5	25.5	0.0
5	45	82.2	17.8	0.0
6	22.5	85.2	14.8	0.0
7	11.25	87.6	12.4	0.0
8	5.63	90.2	9.8	0.0
9	2.81	92.3	7.7	0.0
10	1.41	91.8	8.2	0.0